Ceftriaxone affects ferroptosis and alleviates glial cell activation in Parkinson's disease

HUI ZHI[1*], XIAOYU WANG[2*], YUJIA CHEN[1,3], ZENGLIN CAI[1], JINGWEI LI[1,3] and DONGKAI GUO[1]

[1]Department of Pharmacy, Suzhou Research Center of Medical School, Suzhou Hospital, Affiliated Hospital of Medical School, Nanjing University, Suzhou, Jiangsu 215153, P.R. China; [2]Department of Pharmacy, The Affiliated Suzhou Hospital of Nanjing Medical University, Suzhou Municipal Hospital, Suzhou, Jiangsu 215002, P.R. China; [3]Department of Neurology, Nanjing Drum Tower Hospital Clinical College of Traditional Chinese and Western Medicine, Nanjing University of Chinese Medicine, Nanjing, Jiangsu 210008, P.R. China

Received August 13, 2024; Accepted February 26, 2025

DOI: 10.3892/ijmm.2025.5526

Abstract. Parkinson's disease (PD) is the second most common neurodegenerative disorder, which is characterized by the death of dopaminergic neurons. It has been reported that ceftriaxone (CEF) exerts promising effects on alleviating dopaminergic neuron death in PD models. However, the neuroprotective mechanisms of CEF in PD have not been well understood. In the present study, to investigate the neuroprotective effects of CEF through western blot and immunofluorescence assays, two *in vivo* models were established, namely the 1-methyl-4-phenyl-1,2,3,6-tetrahydropyridine (MPTP)- and lipopolysaccharide (LPS)-induced models. Additionally, three *in vitro* models were used to explore the neuroprotective mechanisms of CEF, namely the 1-methyl-4-phenylpyridinium ion (MPP^+)-induced dopaminergic neuron injury, LPS-induced microglia activation and TNFα-induced astrocyte activation models, with key insights derived from western blot and qPCR experiments. The *in vivo* studies demonstrated that CEF exerted neuroprotective effects and reduced glial cell activation. Additionally, CEF reversed the reduction of tyrosine hydroxylase and suppressed the activation of microglia and astrocytes. Furthermore, the *in vitro* experiments revealed that CEF could display both direct and indirect neuroprotective effects and could directly alleviate MPP^+-induced neuronal toxicity and suppress the activation of microglia and astrocytes. In addition, CEF indirectly reduced neuronal injury caused by conditioned medium from activated microglia and astrocytes. Mechanistic studies revealed that CEF inhibited the ferroptosis pathway via regulating the expression of solute carrier family 7 member 11 and glutathione peroxidase 4 in a non-cell-specific manner. Via inhibiting ferroptosis, CEF could directly protect dopaminergic neurons and prevent glial cell activation, and indirectly impair neurons. In conclusion, the results of the current study highlighted the potential research and therapeutic value of CEF in regulating ferroptosis in PD.

Correspondence to: Dr Dongkai Guo, Department of Pharmacy, Suzhou Research Center of Medical School, Suzhou Hospital, Affiliated Hospital of Medical School, Nanjing University, 1 Lijiang Road, Suzhou, Jiangsu 215153, P.R. China
E-mail: dongkaiguo@126.com

*Contributed equally

Key words: Parkinson's disease, ceftriaxone, neuroinflammation, ferroptosis, glutathione peroxidase 4, solute carrier family 7 member 11, microglia, astrocyte

Introduction

Parkinson's disease (PD) is a prevalent degenerative disease of the central nervous system (CNS), significantly affecting the quality of life through both motor and non-motor symptoms (1). The primary pathological features of PD include the progressive loss of dopaminergic neurons in the substantia nigra (SN) pars compacta and the formation of Lewy bodies, composed of α-synuclein (α-syn) (2). It has been reported that factors, such as α-syn aggregation, oxidative stress, ferroptosis, mitochondrial dysfunction, neuroinflammation and gut dysbiosis are involved in the degeneration and death of dopaminergic neurons in PD (3). Although levodopa is commonly used as a first-line therapy to alleviate motor symptoms, it cannot halt the progression of PD (4). Therefore, developing interventions to slow or stop the progression of PD remains a top priority for both patients and researchers (5).

Ceftriaxone (CEF), a third-generation cephalosporin antibiotic, has shown neuroprotective effects in recent studies on PD. In a 1-methyl-4-phenyl-1,2,3,6-tetrahydropyridine (MPTP)-induced PD animal model, CEF was found to reverse behavioral deficit and promote neurogenesis (6,7). It could also mitigate nigral oxidative damage and enhance neurogenesis (8), reduce glutamate-mediated neuro-inflammation and restore brain-derived neurotrophic factor (BDNF) levels (9). At the molecular level, CEF could bind to α-syn to inhibit its polymerization *in vitro* (10). These findings suggested that CEF could be applied in the treatment of PD. However, the particular neuroprotective mechanisms of CEF remain unclear. Emerging evidence has indicated that ferroptosis is a key molecular mechanism in PD (11). Since cystine/glutamate transport is closely associated with ferroptosis and CEF can

regulate glutamate transport, it was hypothesized that CEF could affect PD via modulating ferroptosis.

The current study aimed to investigate the ferroptosis-related neuroprotective mechanism of CEF and neuroinflammation in PD. Therefore, both *in vivo* and *in vitro* PD injury models were established to verify whether CEF could alleviate glial cell activation and neuronal damage in PD via inhibiting ferroptosis.

Materials and methods

Cell culture and drugs. BV2 (cat. no. SCSP-5208; Cell Bank of Type Culture Collection of the Chinese Academy of Sciences) and C8-D1A [cat. no. CRL-2541; American Type Culture Collection (ATCC)] cells were cultured in DMEM (Gibco; Thermo Fisher Scientific, Inc.), while SH-SY5Y cells (cat. no. CRL-2266; ATCC) in DMEM/F12, both supplemented with 10% heat-inactivated fetal bovine serum (both from Gibco; Thermo Fisher Scientific, Inc.) and penicillin/streptomycin solution (100 μg/ml) at 37˚C in a humidified incubator with 5% CO_2. CEF (Roche Diagnostics) and MPP^+ (MedChemExpress) were dissolved in saline and DMSO, respectively. Liposaccharide (LPS; MilliporeSigma), MPTP (MedChemExpress) and TNFα (Beyotime Institute of Biotechnology) were dissolved in saline. Cells were seeded into 12-well plates starting at a concentration of $2x10^5$ cells/ml and incubated overnight. Cells in the experimental group were pre-treated with 300 μM CEF for 4 h with a confluency of ~75% at the time of treatment. For inflammatory activation, BV2 and C8-D1A cells were challenged with 100 ng/ml LPS and 10 ng/ml TNFα, respectively, for 24 h. To establish the MPP^+-induced SH-SY5Y cell model, cells were treated with 1 μM MPP^+ for 24 h.

Antibodies. Immunoblot analysis was performed using the following primary antibodies: Anti-tyrosine hydroxylase (TH; 1:2,000; cat. no. 25859-1-AP), anti-solute carrier family 7 member 11 (SLC7A11; 1:1,000; cat. no. 26864-1-AP), anti-glial fibrillary acidic protein (GFAP; 1:10,000; cat. no. 60190-1-Ig; all from Proteintech Group, Inc.), anti-cyclooxygenase-2 (COX-2, 1:1,000; cat. no. ab179800), anti-inducible nitric oxide synthase (iNOS; 1:1,000; cat. no. ab178945), anti-glutathione peroxidase 4 (GPX4; 1:2,000; cat. no. ab125066,), anti-allograft inflammatory factor 1 (IBA1; 1:1,000; cat. no. ab178846; all from Abcam), anti-GAPDH (1:1,000; cat. no. 5174S), anti-p65 (1:1,000; cat. no. 8242S) and anti-phosphorylated (p)-p65 (1:1,000; cat. no. 3033S; all from Cell Signaling Technology, Inc.). Horseradish peroxidase (HRP)-conjugated goat anti-mouse (1:10,000; cat. no. 31430) or anti-rabbit antibodies (1:10,000; cat. no. 31460; Thermo Fisher Scientific, Inc.) served as secondary antibodies. The proteins were visualized using an ECL detection kit (Thermo Fisher Scientific, Inc.).

Animal study. C57BL/6 mice (male, n=72, weight, 25-30 g) were purchased from Shanghai Slack Laboratory Animal Co., Ltd. Each group was comprised six mice. All mice were maintained under controlled temperature (22±1˚C) and humidity (50±5%) conditions in a 12/12-h light/dark cycle with free access to food and water. The PD mouse model was established by intraperitoneal injection of 5 mg/ml MPTP (dissolved in saline) for 7 days (25 mg/kg per day for the first three days followed by 30 mg/kg per day for the last 4 days). No mice succumbed after MPTP injection in the present experiment. After the 7-days period of continuous injections of MPTP, a behavioral test was conducted to confirm the establishment of a stable pathological state in the mice. To assess the successful establishment of the PD model, mice were subjected to a series of behavioral tests, including the rotarod and climbing rod tests. Only mice with significant motor deficits were selected for the subsequent experiments. A total of 12 mice were selected for the study, and the remaining mice were euthanized according to the protocol approved by the Institutional Animal Care and Use Committee. The neuroinflammatory *in vivo* model was established following stereotaxic injection of 1 mg/ml lipopolysaccharide (LPS; volume, 2 μl) into the ventricles. Pentobarbital sodium was administered at a dose of 50 mg/kg to anesthetize the mice prior to the injection. Mice in the CEF and blank control groups were intraperitoneally injected for 7 days with 200 mg/kg CEF (once a day) and equal volume of saline, respectively. After the experiment, mice were anesthetized by pentobarbital sodium and then euthanized by cervical dislocation. Mouse brain slices were collected for western blot and immunohistochemistry assays. All experimental operations in animals were performed simultaneously according to the Institutional Guidelines for Animal Use and Care and all procedures were approved by the Animal Committee of Suzhou Institute of Biomedical Engineering and Technology, Chinese Academy of Sciences (approval no. 2024-A50; Suzhou, China). For the MPTP-treated C57BL/6 mouse model of PD, humane endpoints were defined as follows: Severe weight loss (a reduction of 20% or more from baseline weight), severe neurological impairment (including inability to move, tremors, or non-response to being placed on their back), severe pain or distress (indicated by labored breathing, extreme dehydration, or abnormal posture), lack of appetite and water consumption (evidenced by signs of dehydration or malnutrition), severe tremors or convulsions that impede overall well-being, and unhealed injuries or wounds resulting in infection or extreme pain. If any mice exhibited these symptoms, humane euthanasia would be conducted to prevent prolonged suffering. In the present study, all mice were euthanized before the conclusion of the experiment; however, none of the mice reached these humane endpoints.

Behavioral tests. Rotarod and climbing rod tests are commonly used to assess motor coordination and bradykinesia in animal models of neurological disorders (12,13). The behavioral instruments were purchased from SANS Biological Technology (https://www.sansbio.com). Rotarod test: Mice were trained on the rotarod until they could remain on it for over 2 min at a speed of 4 revolutions per min (r/min) during the training. On the day of testing, the speed of the rotarod was gradually increased from 4 to 40 r/min over 5 min. Each mouse was monitored freely walking on the rotarod, and the elapsed time until falling was recorded. This experiment was conducted three times per mouse. Pole test: A wooden pole with a rough surface, measuring 50 cm in height and 1 cm in diameter, was inserted into the home cage. During the training session, every mouse was positioned on top of the pole and allowed to descend to the home cage from the peak three

times. On the day of testing, each mouse was placed head-first on top of the pole, and the duration taken for it to descend back into the cage was timed. The experimentation process was conducted thrice for every mouse.

Western blot analysis. Total proteins were extracted from tissues or cells using a RIPA lysis solution supplemented with protease inhibitors (both from Beyotime Institute of Biotechnology). Protein quantification was performed using a BCA protein quantification kit (Beyotime Institute of Biotechnology). Subsequently, ~30 μg protein extracts were separated by 8-12% SDS-PAGE and were then transferred onto a PVDF membrane (MilliporeSigma). Following transfer, the membranes were subjected to blocking with 5% (w/v) skim milk powder diluted in Tris-buffered saline containing 0.1% Tween-20 (TBST) under ambient conditions (25±2˚C) for 1 h. The membranes were first incubated with primary antibodies at 4˚C overnight in a refrigerator and then with the corresponding secondary antibody at room temperature for 2 h. The blots were then incubated with an ECL reagent and the expression levels of the target proteins were detected using a chemiluminescence imaging analysis system (Clinx Science Instruments Co., Ltd.). GAPDH was used as a reference gene. Quantification was performed with ImageJ software (version 1.54k; National Institutes of Health).

Immunofluorescence staining. The brains of mice were injected with 4% paraformaldehyde (PFA), fixed in 4% PFA at 4˚C for three days and were then incubated with 30% sucrose at 4˚C for three days. Subsequently, the 20-μm thick brain sections were collected and incubated with 5% fetal bovine serum (cat. no. Gibco-10270-106; Thermo Fisher Scientific, Inc.) to block non-specific protein binding. The tissue sections were then incubated at 4˚C overnight with the primary antibodies. After washing the tissue sections with PBS on a decolourisation shaker, they were incubated with the corresponding secondary antibodies Alexa Fluor 488 (1;500; cat. no. A-21202) and Alexa Fluor 594 (1:500; cat. no. A-21207) from Invitrogen (Thermo Fisher Scientific, Inc.) at room temperature for 1 h. Subsequently, the sections were examined using an inverted fluorescence microscope (IX71; Olympus Corporation). For cell counts and quantitative statistics for fluorescence intensity, ImageJ software was used.

Cell viability assay. The Cell Counting Kit-8 (CCK-8) assays were performed according to the manufacturer's instructions. Briefly, cells were seeded in a 96-well plate at a concentration of $1x10^5$ cells/well and allowed to adhere overnight. Following treatment with increasing concentrations of the indicated drugs for 24 h, each well was supplemented with 10 μl CCK-8 solution (cat. no. C0039; Beyotime Institute of Biotechnology). The plate was incubated at 37˚C for 2 h and the absorbance in each well was measured at a wavelength of 450 nm using a microplate reader (CMaxPlus from Molecular Devices, LLC).

Reverse transcription-quantitative PCR (RT-qPCR). Total RNA was isolated from cells using TRIzol reagent (Invitrogen; Thermo Fisher Scientific, Inc.). cDNA was reversely transcribed from total RNA using PrimeScript RT Master Mix (Takara Bio, Inc.) following the manufacturer's instructions. qPCR was performed using a LightCycler 480 system (Roche Diagnostics) with TB Green® Premix Ex Taq™ II (Takara Bio, Inc.). The thermal cycling protocol comprised an initial denaturation step at 95˚C for 30 sec, followed by 40 cycles of denaturation at 95˚C for 5 sec and combined annealing/extension at 60˚C for 10 sec. RT-qPCR analysis was performed using the $2^{-\Delta\Delta Cq}$ method (14). RT-qPCR primers were designed as follows: mouse iNOS forward, 5'-TCCCAGCCTGCCCCTTCAAT-3' and reverse, 5'-CGGATCTCTCTCCTCCTGGG-3'; COX-2 forward, 5'-CAGGCTGAACTTCGAAACAG-3' and reverse, 5'-CTCACGAGGCCACTGATACCTA-3'; and β-actin forward, 5'-GACCTGACTGACTACCTC-3' and reverse, 5'-GACAGCGAGGCCAGGATG-3'.

Conditioned media (CM). BV2 cells were pretreated with or without CEF (300 μM) for 4 h and then exposed to LPS (100 ng/ml) for 24 h. C8-D1A cells were pretreated with or without CEF (300 μM) for 4 h and then exposed to TNFα (10 ng/ml) for 24 h. CM was used to culture SH-SY5Y cells.

Data analysis. Prism version 7.0 (GraphPad Software; Dotmatics) was used for data analysis. Statistical analysis was conducted by one-way analysis of variance (ANOVA) followed by Tukey's post hoc test for multiple comparisons, as indicated in the figure legends. The data are presented as the mean ± standard deviation (SD). $P<0.05$ was considered to indicate a statistically significant difference.

Results

CEF displays a direct protective effect on neurons via reversing the expression of TH in a MPTP-induced mouse model. TH is a rate-limiting enzyme, which is involved in the synthesis of dopamine, while it is widely acknowledged as a marker of dopaminergic neurons, which transport dopamine from the SN to the caudal putamen (CPu) via the nigro-striatum pathway (15). Dopamine is synthesized in dopaminergic neurons in the SN and then transmitted through synapses to different brain regions such as CPu, which receives a large amount of dopamine input from SN (16). Therefore, it can be observed that both the SN and CPu are capable of detecting the presence of TH. To evaluate the effect of CEF on PD neuropathology, western blot and immunofluorescence analyses were carried out to detect the expression levels of TH in both the SN and CPu in a MPTP mice model. C57BL/6 mice were administered CEF with intraperitoneal injections after intraperitoneally administering MPTP (Fig. 1A). Behavioral tests demonstrated that the MPTP-treated mice had a significant decrease in latency time on the rotarod and increase in pole test time, indicating a decline in their motor coordination abilities (Fig. 1B and C). Western blot analysis revealed that CEF could significantly reverse the MPTP-induced TH downregulation in the SN and CPu (Fig. 1D-G). Additionally, immunofluorescence analysis revealed that CEF could substantially alleviate the loss of MPTP-induced TH immunoreactive neurons in the SN and CPu (Fig. 1H-K). These findings suggested that treatment with CEF could promote neuronal protection in a PD mouse model.

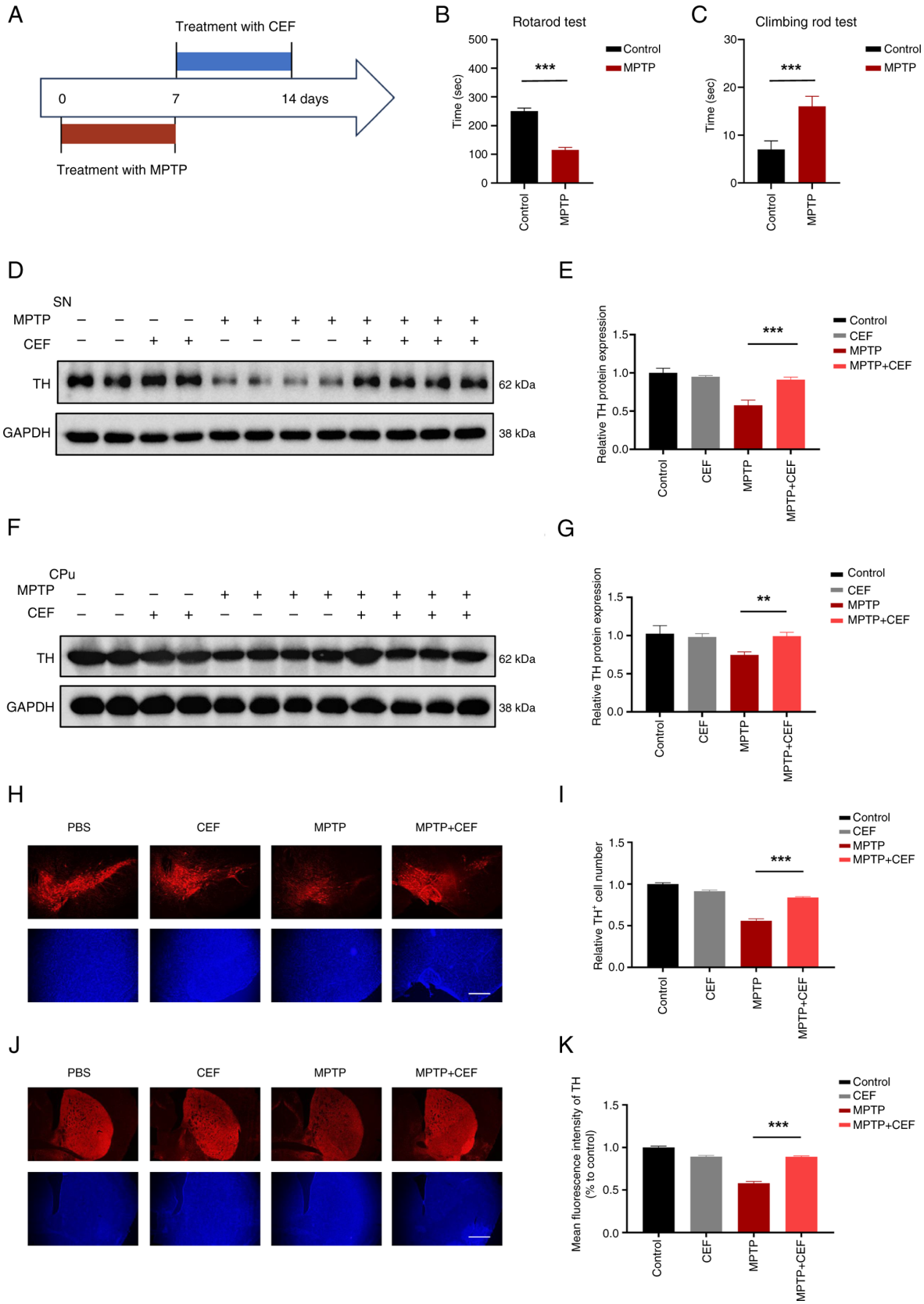

Figure 1. CEF reverses the expression of TH in a MPTP-induced mouse model. (A) Experimental design of CEF treatment in attenuating Parkinson's disease in a mouse model. Mice were intraperitoneally injected with MPTP once a day for 7 days (25 mg/kg for the first 3 days, 30 mg/kg for the last 4 days), followed by intraperitoneal injection of 200 mg/kg CEF once a day for 7 days. (B) Latencies to fall from the accelerated rotating beams in the rotarod tests. (C) Climbing time on climbing rod tests. (D) The protein expresion levels of TH were detected in the SN of brain tissue sections using western blot analysis. (E) The protein expression levels of TH in (D) were quantified following normalization to those of GAPDH. (F) The protein expression levels of TH were also detected in the CPu region of the brain by western blot analysis. (G) The protein expression levels of TH in (F) were quantified after normalization to the expression levels of GAPDH. (H-K) The brain tissue sections were cut into slices and stained with an antibody against TH. The corresponding fluorescence images and statistical analysis of TH expression in (H and I) the SN and (J and K) CPu are presented. Data are expressed as the mean ± SD. **P<0.01 and ***P<0.001 (n=3). Scale bar, 100 μm. Coronal slices. CEF, ceftriaxone; TH, tyrosine hydroxylase; MPTP, 1-methyl-4-phenyl-1,2,3,6-tetrahydropyridine; SN, substantia nigra; CPu, caudal putamen.

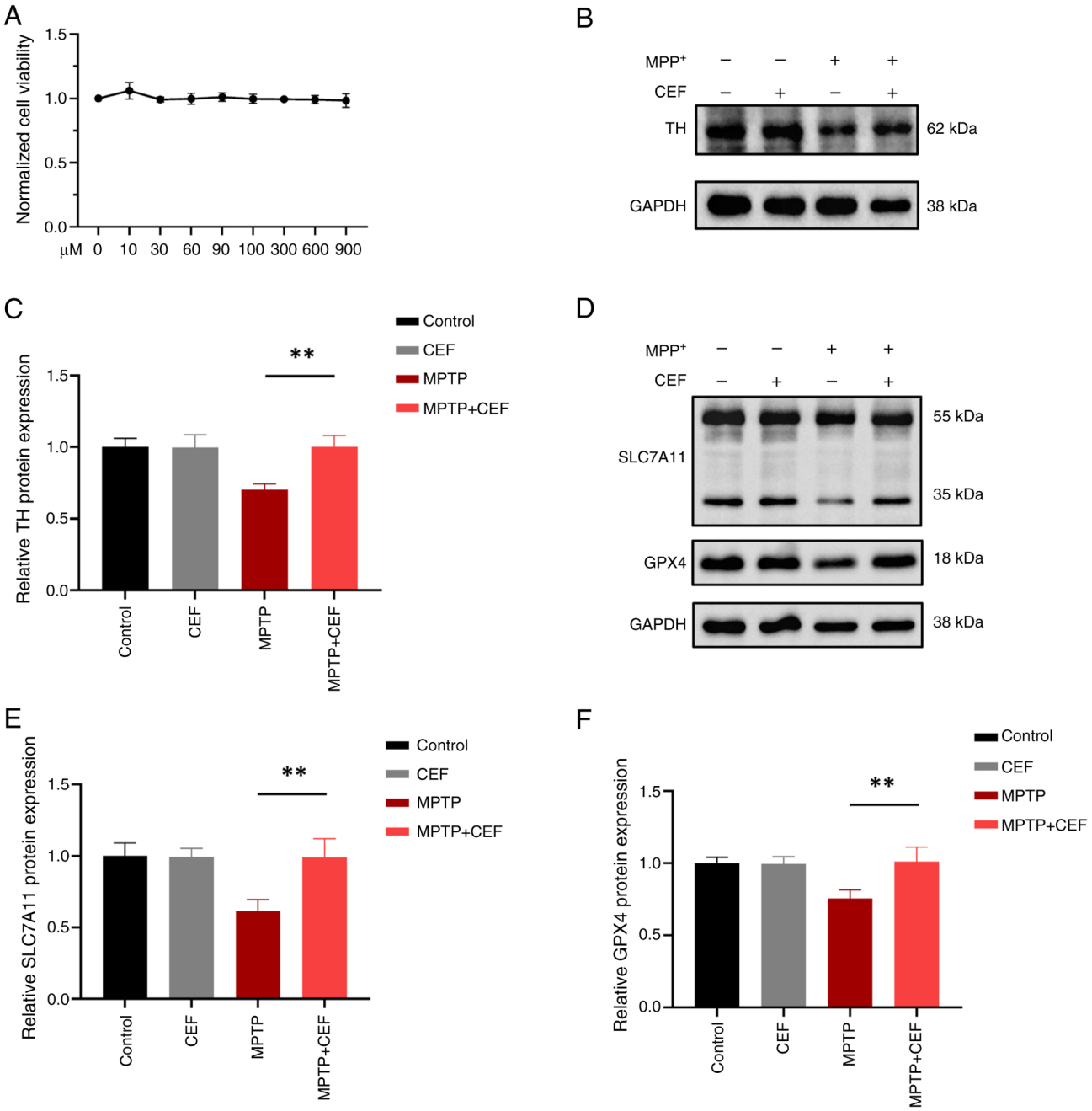

Figure 2. CEF reverses TH expression and inhibits ferroptosis in MPP+-induced SH-SY5Y cells. (A) A Cell Counting Kit-8 assay was performed to assess the effect of CEF on cell viability. SH-SY5Y cells were treated with different CEF concentrations (0-900 μM) for 24 h. (B) SH-SY5Y cells were pre-treated with CEF (300 μM) for 4 h. Subsequently, cells were treated with 1 μM MPP+ for an additional 24 h and the protein expression levels of TH were detected by western blot analysis. (C) The relative protein expression levels of TH were normalized to those of GAPDH. (D) The protein expression levels of SLC7A11 and GPX4 were determined using western blot analysis. Due to the proximity in molecular weight between SLC7A11/GPX4 and GAPDH, simultaneous detection on the same membrane was not feasible, but all experiments utilized the same biological samples and were conducted from the same batch on the same day. (E and F) The relative protein expression levels are shown. Data are presented as the mean ± SD. **P<0.01 (n=3). CEF, ceftriaxone; TH, tyrosine hydroxylase; MPP+, 1-methyl-4-phenylpyridinium ion; SLC7A11, solute carrier family 7 member 11; GPX4, glutathione peroxidase 4.

CEF alleviates MPP+-induced SH-SY5Y cell injury via resisting ferroptosis. The cystine/glutamate antiporter SLC7A11 (xCT)/GPX4 system is considered as the mainstay to inhibit ferroptosis, since glutathione (GSH) is the principal antioxidant in mammalian cells (17). To explore the neuroprotective mechanism in neurons, the effect of the SLC7A11/GPX4 axis in the ferroptosis pathway was investigated. Therefore, the effect of different concentrations of CEF on SH-SY5Y cell viability was assessed by CCK-8 assay. The results identified that CEF at a concentration of 900 μM had no toxic effect on the viability of SH-SY5Y cells (Fig. 2A). In addition, western blot analysis demonstrated that CEF significantly reversed the reduced expression levels of TH in MPP+-induced SH-SY5Y cells (Fig. 2B and C). Additionally, CEF substantially alleviated the MPP+-induced SLC7A11 and GPX4 downregulation in SH-SY5Y cells (Fig. 2D-F). These findings suggested that CEF could suppress ferroptosis via regulating the SLC7A11/GPX4 axis in neurons.

CEF attenuates the activation of microglia and astrocytes in LPS- and MPTP-induced mouse models. Activation of glial cells is accompanied by morphological changes; proinflammatory microglia and astrocytes generally exhibit larger volumes and coarser morphologies, while anti-inflammatory microglia and astrocytes typically feature smaller volumes and more prominent morphologies (18,19). To investigate whether neuroinflammation could be involved in the neuroprotective effects of CEF, tissue-section immunofluorescence staining was utilized to determine cellular morphological characteristics. By utilizing a coupling of markers (namely, the microglial activation-associated marker IBA1 and the astrocyte activation-associated marker GFAP) and morphological traits, it was observed that microglia and astrocytes exhibit larger volumes and coarser morphologies in the SN in both models. However, treatment with CEF considerably abrogated this effect (Fig. 3A-C). The same effects were also observed in the CPu of the brain (Fig. 3D-F). The aforementioned results indicated that CEF could attenuate neuroinflammation via inhibiting the activation of microglia and astrocytes *in vivo*.

CEF displays an indirect protective effect on neurons via inhibiting the activation of microglia and astrocytes in the LPS-induced mouse model. Given that CEF inhibited the activation of microglia and astrocytes in both the LPS- and MPTP-induced mouse models, the current study also aimed to explore whether CEF could protect neurons in the LPS-induced mouse model. A pro-inflammatory state can cause changes in an increase in the expression of GFAP in astrocytes and IBA-1 in microglia (20). Western blotting was utilized to determine the expression of GFAP and IBA-1. The western blot analysis results revealed a significant induction in IBA1 and GFAP expression accompanied by a considerable reduction in TH expression in LPS-induced mice. However, treatment with CEF reversed the aforementioned changes (Fig. 4A-D). Furthermore, immunofluorescence analysis showed that CEF considerably attenuated the loss of TH immunoreactive neurons in mice treated with LPS (Fig. 4E-H). Overall, these data suggested that CEF could supress neuroinflammation and inhibit neuroinflammation-mediated neurotoxicity *in vivo*.

CEF inhibits neurotoxicity via attenuating microglial activation. The aforementioned *in vivo* studies demonstrated that CEF could inhibit glial cell activation and alleviate neuronal injury. Therefore, subsequently, *in vitro* studies were preformed to investigate this mechanism. CCK-8 assays showed that CEF at a concentration of 900 μM had no toxic effect on BV2 cell viability (Fig. 5A). In addition, the mRNA and protein expression levels of iNOS and COX-2 were significantly increased in LPS-treated BV2 cells. However, cell pre-treatment with CEF considerably reversed this effect (Fig. 5B-D), thus suggesting that CEF could alleviate microglial activation. Nuclear factor-κB (NF-κB) is a key transcription factor involved in regulating the expression of inflammatory genes, while the increased phosphorylation of NF-κB/p65 is a primary trigger for inflammatory activation (21). In the present study, the results demonstrated that p-NF-κB/p65 was upregulated, while its expression levels were decreased following cell pre-treatment with CEF (Fig. 5E and F). The aforementioned finding indicated that CEF could alleviate microglial activation via regulating the NF-κB pathway. Emerging evidence has suggested that the activation of inflammation promotes ferroptosis (22,23). Therefore, whether the ferroptosis mechanism could be associated with the CEF-mediated inhibition of microglial activation was also explored. The western blot analysis results demonstrated that CEF could significantly reverse the loss of SLC7A11 and GPX4 protein expression levels in LPS-treated BV2 cells (Fig. 5G and H). These findings suggested that CEF could suppress ferroptosis via regulating the SLC7A11/GPX4 axis in activated microglia. Subsequently, whether microglial activation could affect neuronal survival was determined. Therefore, the conditioned medium (CM) from LPS-treated BV2 cells induced cellular injury in SH-SY5Y cells, a neuroblastoma cell line. Additionally, the CM from LPS-treated BV2 cells pre-treated with CEF reduced cellular toxicity in SH-SY5Y cells (Fig. 5I and J). Collectively, these findings suggested that CEF could inhibit microglial activation *in vitro* and protect neurons from microglial activation-induced neuronal damage.

CEF inhibits neurotoxicity via alleviating astrocyte activation. To further investigate the role of CEF in astrocyte activation, further *in vitro* studies were carried out in TNFα-treated C8-D1A cells. The CCK-8 assay results revealed that C8-D1A cell treatment with 900 μM CEF had no toxic effect on these cells (Fig. 6A). In TNFα-treated C8-D1A cells, CEF significantly reduced the mRNA and protein expression levels of iNOS and COX-2, thus suggesting that CEF could inhibit astrocyte activation (Fig. 6B-D). Additionally, CEF could alleviate the enhanced expression levels of p-NF-κB/p65 in TNFα-treated C8-D1A cells, thus indicating that CEF could inhibit astrocyte activation via regulating the NF-κB pathway (Fig. 6E and F). Furthermore, the western blot results revealed that CEF could significantly restore the reduced protein expression levels of SLC7A11 and GPX4 in TNFα-treated C8-D1A cells, thus suggesting that CEF could suppress ferroptosis via regulating the SLC7A11/GPX4 axis in activated astrocytes (Fig. 6G and H). In addition, CM from TNFα-treated C8-D1A cells pre-treated with CEF reduced cellular toxicity in SH-SY5Y cells (Fig. 6I and J). Overall, the aforemetioned findings suggested that CEF could inhibit astrocyte activation and protect neurons against astrocyte activation-induced neuronal death *in vitro* (Fig. 7).

Discussion

Neuroinflammation is an early and persistent phenomenon in PD, which is commonly driven by microglia and astrocytes in the CNS (24). This immune response is crucial for maintaining tissue homeostasis, removing pathogens and recovering from damage (25). The primary feature of PD, α-syn, directly activates microglia, thus leading to increased production of pro-inflammatory cytokines and reactive oxygen species (ROS) (26). It has been reported that cytokines, such as TNFα, released from microglia, can activate neighboring astrocytes (20). A previous study demonstrated that persistent inflammation was involved in α-syn aggregation, while the resulting ROS could lead to lipid peroxidation, thus driving ferroptosis and non-apoptotic cell death (27). It was previously shown that glial activation-induced ferroptosis in neurons is a

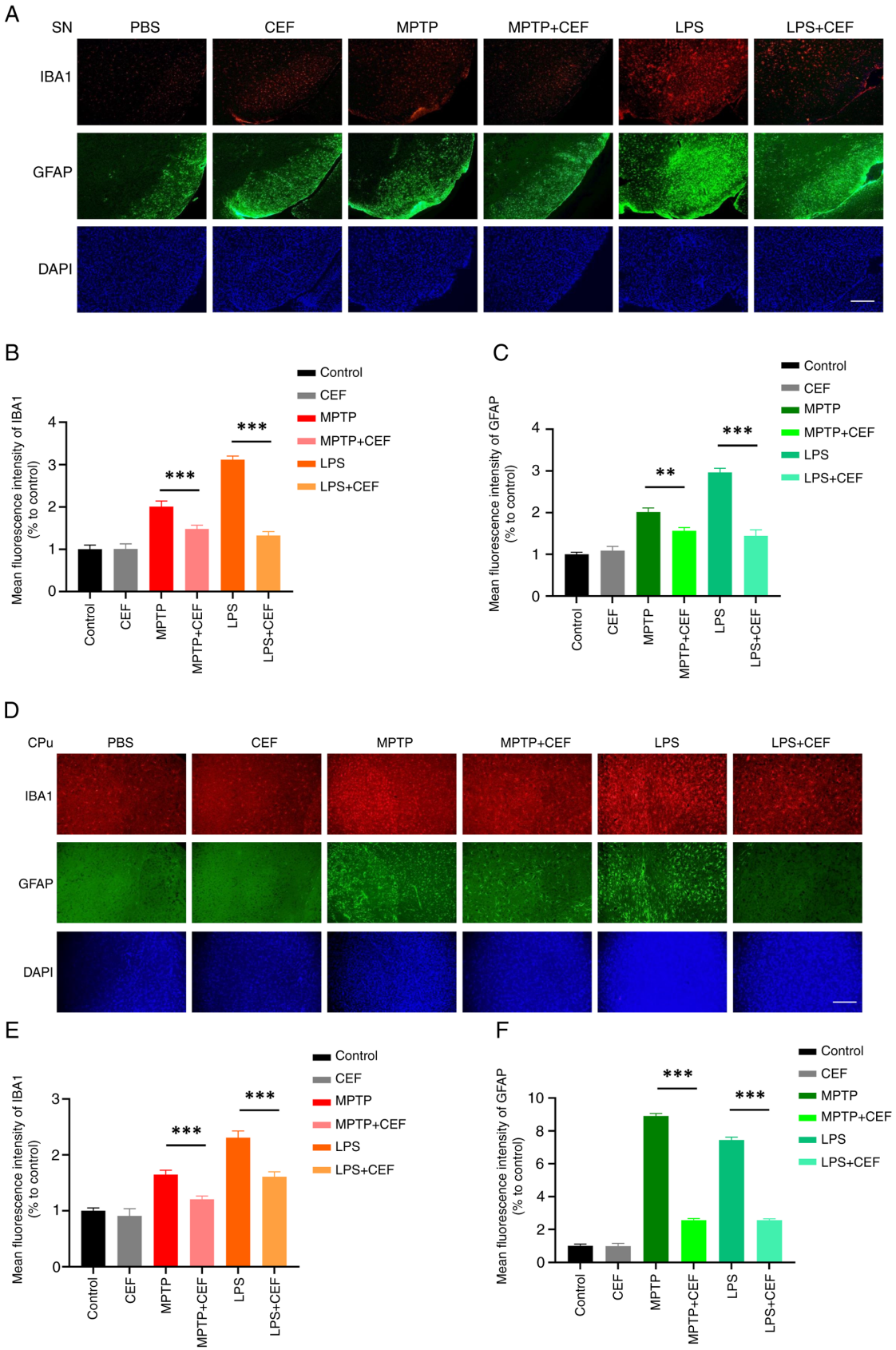

Figure 3. CEF inhibits the activation of glial cells in LPS- and MPTP-treated mice. (A-C) To establish a LPS-induced mouse model, mice were stereotaxically injected with 2 μl LPS (1 mg/ml) into the ventricles, followed by intraperitoneal injection of CEF (200 mg/kg) once a day for 7 days. For the establishment of the MPTP-induced mouse model, mice were intraperitoneally injected with 25 mg/kg MPTP per day for the first 3 days and 30 mg/kg per day for the last 4 days. Subsequently, mice were intraperitoneally injected with 200 mg/kg CEF once a day for 7 days. The brain tissues were cut into slices and stained with antibodies against IBA1 and GFAP. Fluorescence images and statistical analysis of the IBA1 and GFAP protein expression levels in the substantia nigra are shown. (D-F) Fluorescence images and statistical analysis of IBA1 and GFAP expression in the caudal putamen are presented. Data are expressed as the mean ± SD. **P<0.01 and ***P<0.001 (n=3). Scale bar, 100 μm. Coronal slices. CEF, ceftriaxone; LPS, lipopolysacharide; MPTP, 1-methyl-4-phenyl-1,2,3,6-tetrahydropyridine; IBA1, allograft inflammatory factor 1; GFAP, glial fibrillary acidic protein.

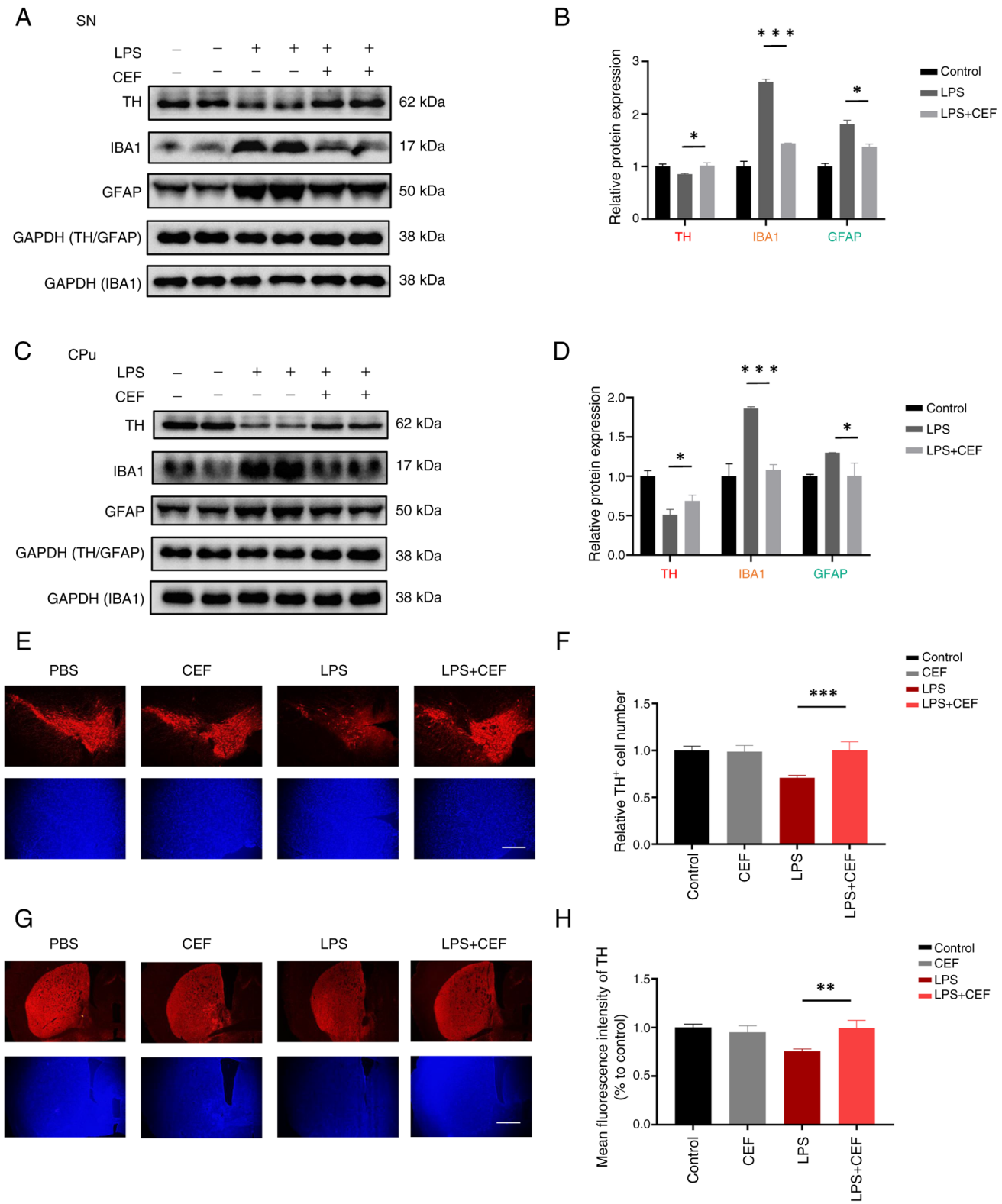

Figure 4. CEF reverses TH expression in LPS-induced mice. (A-D) Mice were stereotaxically injected with 2 μl LPS (1 mg/ml) into the ventricles, followed by intraperitoneal injection of 200 mg/kg CEF once a day for 7 days. The protein expression levels of TH, IBA1 and GFAP were detected in the SN and CPu of the brain by western blot analysis. (E-H) The brain tissues were cut into slices and stained with an antibody against TH. Fluorescence images and statistical analysis of TH expression in the SN and CPu are shown. Data are expressed as the mean ± SD. *P<0.05, **P<0.01 and ***P<0.001 (n=3). Scale bar, 100 μm. Coronal slices. CEF, ceftriaxone; TH, tyrosine hydroxylase; LPS, lipopolysacharide; IBA1, allograft inflammatory factor 1; GFAP, glial fibrillary acidic protein; SN, substantia nigra; CPu, caudal putamen.

key molecular mechanism in PD (11). Ferroptosis, a regulated cell death, which is characterized by overwhelming lipid peroxidation, is closely associated with PD pathogenesis (28). The end-product of ferroptosis, 4-hydroxy-2,3-trans-nonenal, promotes the inflammatory response by α-syn aggregation, indicating that ferroptosis and neuroinflammation potentiate

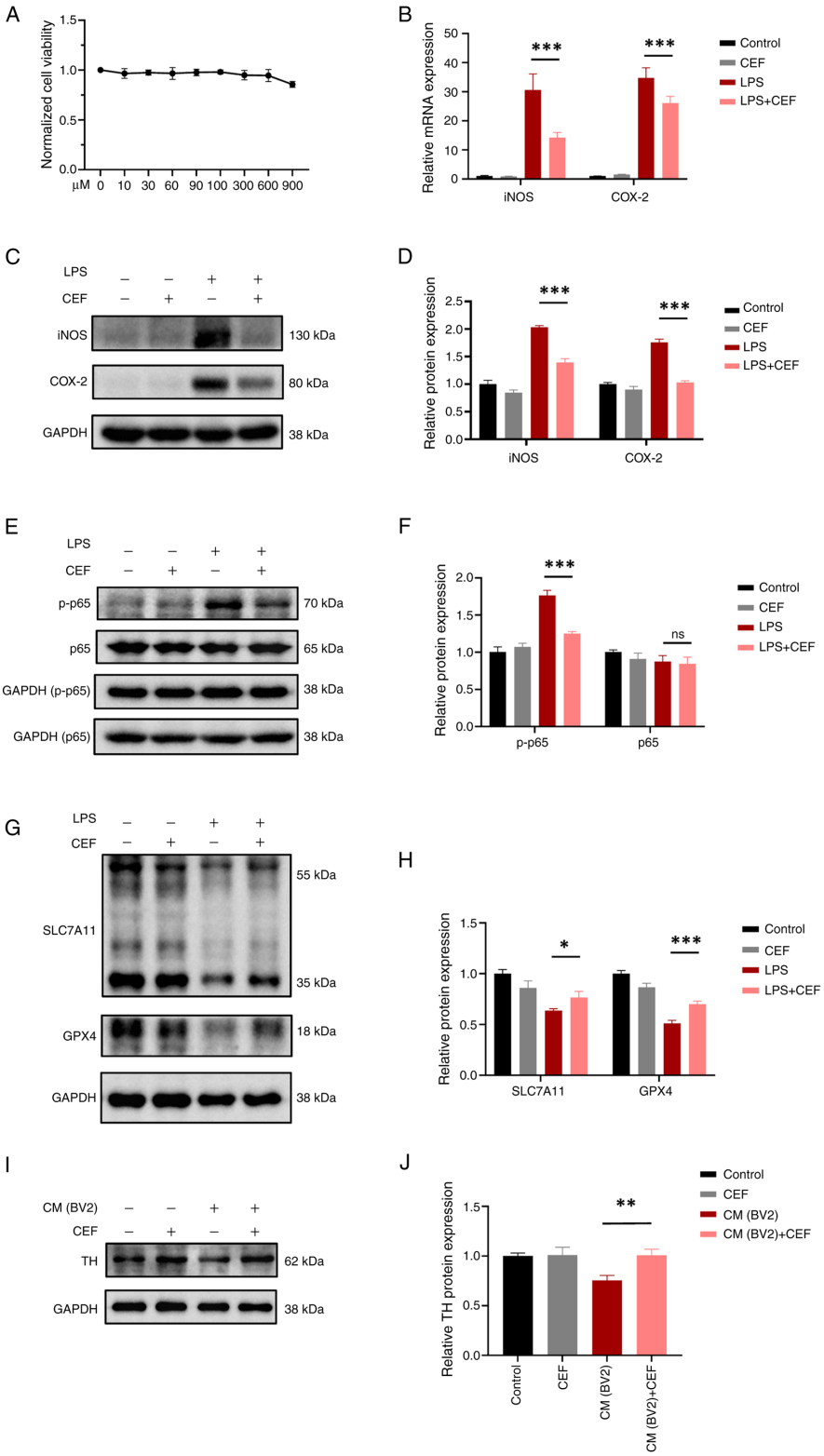

Figure 5. CEF reduces neuronal injury via inhibiting the activation and ferroptosis of microglia. (A) A Cell Counting Kit-8 assay was carried out to examine the effect of CEF on cell viability. BV2 cells were treated with different concentrations of CEF (0-900 μM) for 24 h. (B) BV2 cells were pre-treated with 300 μM CEF for 4 h and then with 100 ng/ml LPS for an additional 6 h. The mRNA expression levels of iNOS and COX-2 were measured by reverse transcription-quantitative PCR. (C) BV2 cells were pre-treated with CEF for 4 h and then with 100 ng/ml LPS for an additional 24 h. Subsequently, the protein expression levels of iNOS and COX-2 were detected by western blot analysis. (D) The relative expression levels of proteins in (C) are shown. (E) BV2 cells were pre-treated with CEF for 4 h and 100 ng/ml LPS for 15 min. Then the protein expression levels of p65 and p-p65 were detected by western blot analysis. (F) The relative expression levels in (E) are shown. (G) BV2 cells were pre-treated with CEF for 4 h. After treatment with 100 ng/ml LPS for 24 h, the protein expression levels of SLC7A11 and GPX4 were measured by western blot assay. Due to the proximity in molecular weight between SLC7A11/GPX4 and GAPDH, simultaneous detection on the same membrane was not feasible, but all experiments utilized the same biological samples and were conducted from the same batch on the same day. (H) The relative expression levels of proteins in (G) are presented. (I) SH-SY5Y were cultured in culture medium from BV2 cells for 24 h and the protein expression levels of TH were detected via western blot analysis. (J) The relative expression levels of proteins in (I) are shown. Data are expressed as the mean ± SD. *P<0.05, **P<0.01 and ***P<0.001 (n=3). CEF, ceftriaxone; LPS, lipopolysacharide; iNOS, inducible nitric oxide synthase; COX-2, cyclooxygenase-2; p-, phosphorylated; SLC7A11, solute carrier family 7 member 11; GPX4, glutathione peroxidase 4; tyrosine hydroxylase.

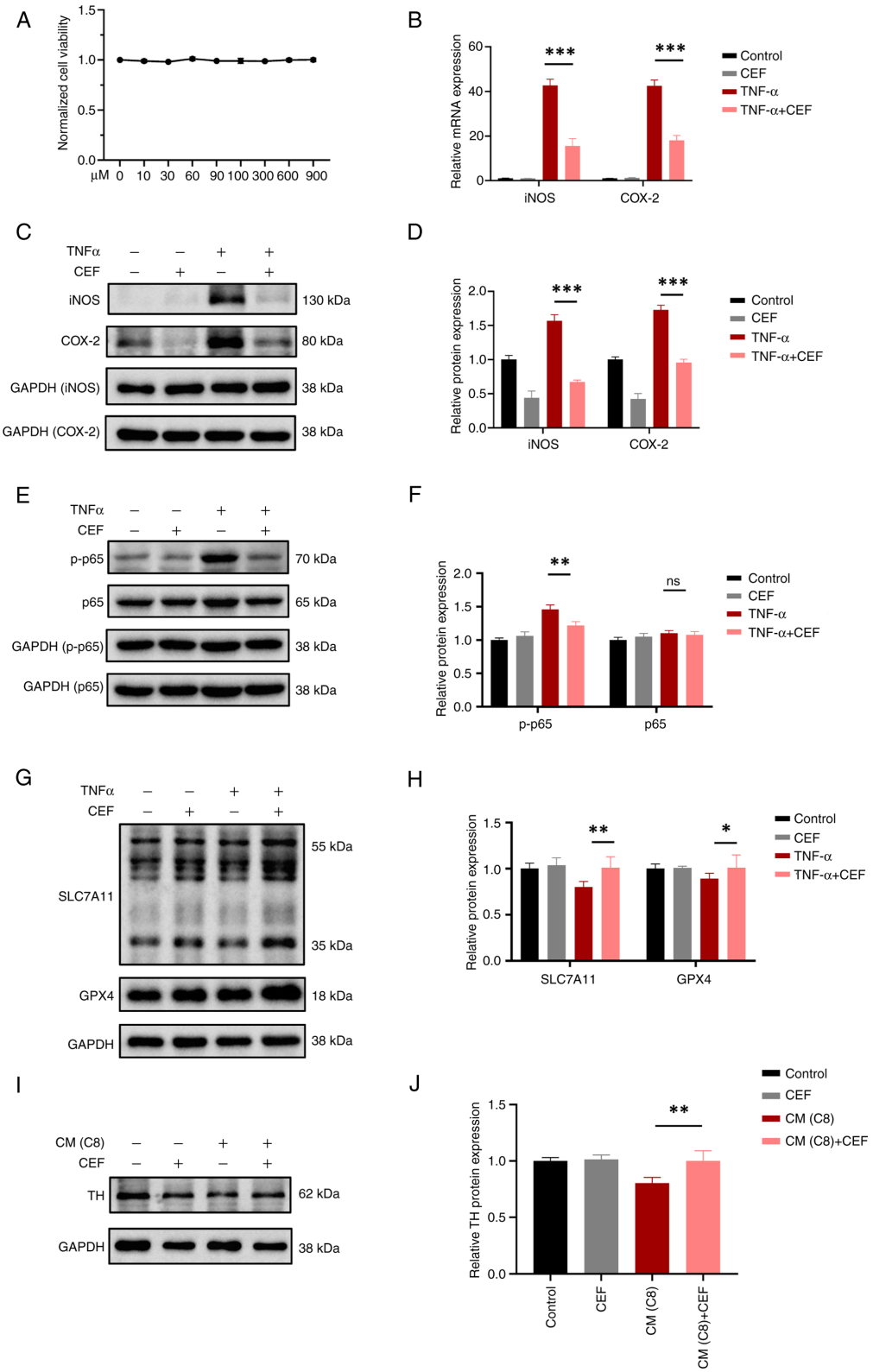

Figure 6. CEF attenuates neuronal injury via inhibiting the activation and ferroptosis of astrocytes. (A) A Cell Counting Kit-8 assay was performed to evaluate the effect of CEF on cell viability. C8-D1A cells were treated with different concentrations of CEF (0-900 μM) for 24 h. (B) C8-D1A cells were pre-treated with 300 μM CEF for 4 h and then with 10 ng/ml TNF-α for an additional 6 h. The mRNA expression levels of iNOS and COX-2 were measured by reverse transcription-quantitative PCR. (C) C8-D1A cells were pre-treated with CEF for 4 h. Following cell treatment with TNF-α (10 ng/ml) for 24 h, the protein expression levels of iNOS and COX-2 were detected by western blot analysis. (D) The relative expression levels of the indicated proteins in (C) are shown. (E) C8-D1A cells were pre-treated with CEF for 4 h. After treatment of cells with 10 ng/ml TNF-α for 15 min, the protein expression levels of p65 and p-p65 were measured by western blot assays. (F) The relative expression levels of the indicated proteins in (E) are presented. (G) C8-D1A cells were pre-treated with CEF for 4 h. Following treatment with TNF-α (10 ng/ml) for 24 h, the protein expression levels of SLC7A11 and GPX4 were measured by western blot analysis. (H) The relative expression levels of the indicated proteins in (G) are shown. (I) SH-SY5Y were cultured in culture medium from C8-D1A cells for 24 h and the protein expression levels of TH were detected using western blot analysis. (J) The relative protein expression levels of TH are presented. Data are expressed as the mean ± SD. *P<0.05, **P<0.01 and ***P<0.001 (n=3). CEF, ceftriaxone; iNOS, inducible nitric oxide synthase; COX-2, cyclooxygenase-2; p-, phosphorylated; SLC7A11, solute carrier family 7 member 11; GPX4, glutathione peroxidase 4; TH, tyrosine hydroxylase; ns, not significant.

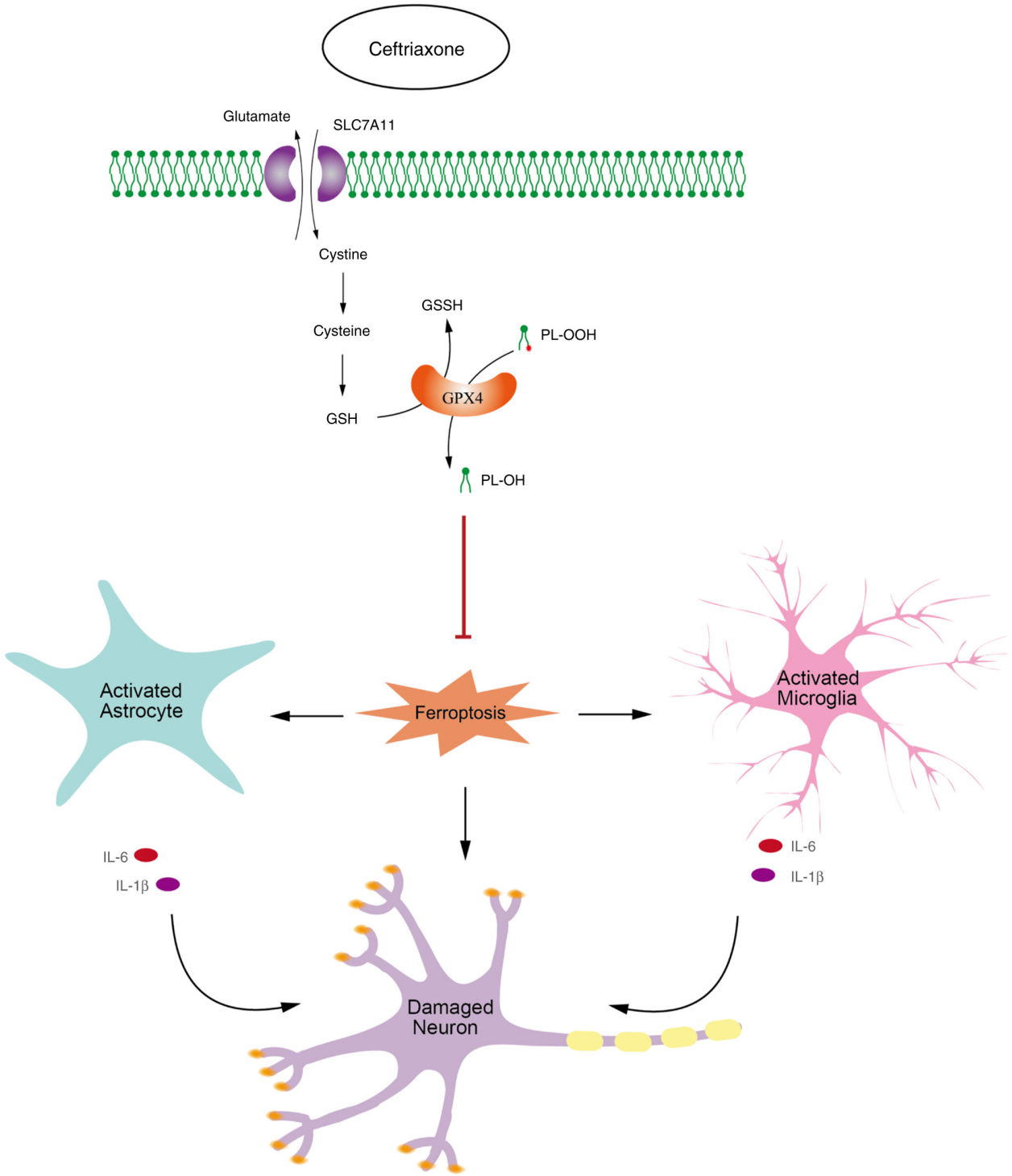

Figure 7. CEF alleviates glial cell activation and neuronal damage via inhibiting ferroptosis. In turn, CEF can inhibit the ferroptosis pathway via regulating the expression levels of SLC7A11 and GPX4 in a non-cell-specific manner, thus directly protecting dopaminergic neurons and preventing glial cell activation, and its indirect effect on damaging neurons. CEF, ceftriaxone; SLC7A11, solute carrier family 7 member 11; GPX4, glutathione peroxidase 4; GSH, reduced glutathione; GSSG, oxidized glutathione; IL, interleukin; PL-OOH, phospholipid hydroperoxides.

each other in PD progression (22). Therefore, regulating inflammation and ferroptosis could offer a potential strategy for treating PD (28,29).

CEF, a third-generation broad-spectrum antibiotic, has been widely used for over 30 years and is generally considered safe (30). In 2005, Rothstein *et al* (31) found that CEF could upregulate astrocytic glutamate transporter-1 (GLT-1) through transcriptional activation. GLT-1 regulates the majority of extracellular glutamate, a significant excitatory neurotransmitter in the CNS (32). Dysregulation of glutamate homeostasis is considered as a core feature of neuropsychiatric disorders (33). Via upregulating GLT-1, CEF could attenuate the behavioral manifestations of various hyper-glutamatergic brain disorders in over 100 preclinical studies (34). In MPTP-induced PD animal models, CEF could reverse behavioral deficits, possibly due to GLT-1 upregulation and its antioxidant and

anti-inflammatory properties, as well as the attenuation of neuronal toxicity mediated by BDNF restoration (6-9). Furthermore, CEF has been recognized to upregulate the glutamate/cystine antiporter (SLC7A11/xCT), which imports cystine in exchange for intracellular glutamate (35-37). This exchange can promote glutamate homeostasis and increase antioxidant activity in astrocytes via promoting the synthesis of GSH, the principal antioxidant in mammalian cells (38). Using GSH as the preferred substrate, GPX4 can convert phospholipid hydroperoxides into non-toxic lipid alcohols, while oxidizing GSH to oxidized glutathione (39). GPX4 is considered as the hub of lipid oxidation, ferroptosis, disease and treatment (40). The SLC7A11/GSH/GPX4 axis, dependent on the cystine-glutamate antiporter system, is considered the mainstay restricting ferroptosis (17). However, whether ferroptosis is associated with the SLC7A11/GPX4 axis in the neuroprotective mechanism of CEF remains poorly understood.

The current study revealed that CEF exerted neuroprotective properties via inhibiting ferroptosis in PD. The results showed that CEF inhibited ferroptosis in both neuronal injury models (Fig. 2D) and glial cell activation *in vitro* models (Figs. 5G and 6G). Since the term was coined in 2012, the research field of ferroptosis has increased exponentially (41). The underlying pathogenesis of PD based on ferroptosis could offer potential therapeutics for this disease (42,43). Previous studies on CEF focused on the role of GLT-1 in PD (43-45). GLT-1 and SLC7A11 could promote glutamate homeostasis via regulating its flow into and out of cells (32,38). Although previous studies demonstrated that CEF upregulated SLC7A11 in APP/PS1 Alzheimer's disease mice and in rats exposed to ethanol (35,36), whether SLC7A11-related ferroptosis is involved in the neuroprotective mechanism of CEF in PD remains poorly understood. A previous *in vitro* study indicated that pre-treatment of PC12 cells with 100 μM CEF could protect them against 6-hydroxydopamine-induced injury (10). Additionally, 100 μM CEF could alleviate MPP^+-induced neurotoxicity in astrocytes (46) and increase SLC7A11 activity, which was associated with GSH levels in HT22 cells treated with 300 μM CEF for 7 days (37). In the present study, the neuroprotective mechanism of CEF (300 μM) and its association with ferroptosis was investigated. The results revealed that CEF inhibited the ferroptosis pathway via regulating SLC7A11 expression in a non-cell-specific manner. Additionally, CEF could block ferroptosis via regulating GPX4, the hub of ferroptosis. The aforementioned findings highlighted the potential research and therapeutic value of CEF in regulating ferroptosis in PD through the SLC7A11/GPX4 axis.

Previous studies also showed that CEF downregulated GFAP and IBA1, thus supporting its potential effect on modulating neuroinflammation in PD rats (47). The MPTP-induced PD model is a recognized and reproducible L-dopa-responsive lesion in the nigrostriatal system, since it can accurately recapitulate several of the key features of the pathophysiology of PD, including the loss of dopaminergic neurons, mitochondrial dysfunction and motor deficits (48,49). The present experiment was designed based on previous literature and laboratory experience, administering MPTP at a dose of 20-30 mg/kg by intraperitoneal injection over 1 week (50,51). Following the MPTP injections, behavioral tests were conducted, such as the rotating rod test and climbing rod test, to screen for successful PD models (12,13). To ensure the precision and reliability of our experimental data, mice of the same birthdate, sex and strain were selected to minimize the influence of individual differences. The present study verified that treatment with CEF could promote neuronal protection in a PD mouse model (Fig. 1). Furthermore, MPTP administration could promote the production of ROS and pro-inflammatory cytokines, which in turn could exacerbate the loss of dopaminergic neurons and motor impairments in mice via promoting oxidative stress and neuroinflammation (52). LPS is a component of the outer membrane of gram-negative bacteria and is used to induce neuroinflammation in PD models. LPS-induced inflammation has been extensively used to study the mechanisms of neuroinflammation in PD, since the activation of microglia can lead to the production of inflammatory cytokines and oxidative stress, which in turn cause dopaminergic neuron death and motor deficits in mice (53). Both the MPTP and LPS-induced PD models are widely used due to their ability to closely mimic several of the key features of PD. The results of present study verified the anti-inflammatory effects of CEF in LPS-induced inflammation models (Figs. 3 and 4A-D). Furthermore, CEF alleviated glial cell activation through the NF-κB pathway (Figs. 5C-F and 6C-F) and reduced glial activation-mediated neuronal toxicity (Figs. 5I and 6I). Activated glial cells can release pro-inflammatory cytokines and other neurotoxic agents that can damage surrounding neuronal cells (18,25). Therefore, understanding the crosstalk between glial cells and neurons is essential in developing effective therapeutic interventions for these diseases (54). In future studies, the authors will consider conducting animal behavior tests to evaluate the efficacy of CEF in improving behavioral anomalies in the PD animal model. Given that the role of GLT-1 in PD has been confirmed, the present study mainly focused on the roles of SLC7A11 and related ferroptosis in PD. The association between GLT-1 and SLC7A11 has not been previously investigated. Other studies also suggested that inflammation could lead to ferroptosis via the activation of multiple inflammation-related signaling pathways. The investigation of ferroptosis in inflammation, particularly in microglia-mediated neuroinflammation, remains in its early stages (55). In the present study, the results suggested that CEF could alleviate glial cell activation and inhibit ferroptosis in PD (Figs. 5G and 6G), thus supporting that the association between inflammation and ferroptosis could be a potential research focus.

In summary, the present study suggested that CEF could alleviate glial cell activation and neuronal damage in PD via inhibiting ferroptosis (Fig. 7). CEF could exert a significant potential in mitigating PD pathology and ferroptosis, positioning inflammatory signaling pathways and driving anti-ferroptosis, thus providing a potential strategy for the treatment of PD.

Acknowledgements

Not applicable.

Funding

The present study was supported by the National Natural Science Foundation of China (grant nos. 82001255 and

32300799), the Natural Science Foundation of Jiangsu (grant no. SBK20200213) and the Suzhou Science and Technology Plan Project (grant nos. SKYD2023090, SKYD2023091 and SKYD2023180).

Availability of data and materials

The data generated in the present study may be requested from the corresponding author.

Authors' contributions

DG conceptualized the study. YC supervised the study. HZ, DG and YC performed the experiments. XW performed data analysis. HZ and DG wrote the main manuscript and prepared Figs. 1, 2 and 4-6. YC prepared Fig. 3. XW and DG revised the manuscript. ZC and JL provided revision suggestions and supplemented experiments. All authors read and approved the final version of the manuscript. HZ and DG confirm the authenticity of all raw data.

Ethics approval and consent to participate

The present study was approved by the ethics committee of Suzhou Institute of Biomedical Engineering and Technology, Chinese Academy of Sciences (approval no. 2024-A50; Suzhou, China).

Patient consent for publication

Not applicable.

Competing interests

The authors declare that they have no competing interests.

References

1. Weintraub D, Aarsland D, Chaudhuri KR, Dobkin RD, Leentjens AF, Rodriguez-Violante M and Schrag A: The neuropsychiatry of Parkinson's disease: Advances and challenges. Lancet Neurol 21: 89-102, 2022.
2. Jankovic J and Tan EK: Parkinson's disease: Etiopathogenesis and treatment. J Neurol Neurosurg Psychiatry 91: 795-808, 2020.
3. Dong-Chen X, Yong C, Yang X, Chen-Yu S and Li-Hua P: Signaling pathways in Parkinson's disease: Molecular mechanisms and therapeutic interventions. Signal Transduct Target Ther 8: 73, 2023.
4. Bloem BR, Okun MS and Klein C: Parkinson's disease. Lancet 397: 2284-2303, 2021.
5. Vijiaratnam N, Simuni T, Bandmann O, Morris HR and Foltynie T: Progress towards therapies for disease modification in Parkinson's disease. Lancet Neurol 20: 559-572, 2021.
6. Hsieh MH, Meng WY, Liao WC, Weng JC, Li HH, Su HL, Lin CL, Hung CS and Ho YJ: Ceftriaxone reverses deficits of behavior and neurogenesis in an MPTP-induced rat model of Parkinson's disease dementia. Brain Res Bull 132: 129-138, 2017.
7. Hsu CY, Hung CS, Chang HM, Liao WC, Ho SC and Ho YJ: Ceftriaxone prevents and reverses behavioral and neuronal deficits in an MPTP-induced animal model of Parkinson's disease dementia. Neuropharmacology 91: 43-56, 2015.
8. Bisht R, Kaur B, Gupta H and Prakash A: Ceftriaxone mediated rescue of nigral oxidative damage and motor deficits in MPTP model of Parkinson's disease in rats. Neurotoxicology 44: 71-79, 2014.
9. Kaur B and Prakash A: Ceftriaxone attenuates glutamate-mediated neuro-inflammation and restores BDNF in MPTP model of Parkinson's disease in rats. Pathophysiology 24: 71-79, 2017.
10. Ruzza P, Siligardi G, Hussain R, Marchiani A, Islami M, Bubacco L, Delogu G, Fabbri D, Dettori MA, Sechi M, *et al*: Ceftriaxone blocks the polymerization of α-synuclein and exerts neuroprotective effects in vitro. ACS Chem Neurosci 5: 30-38, 2014.
11. Wang ZL, Yuan L, Li W and Li JY: Ferroptosis in Parkinson's disease: Glia-neuron crosstalk. Trends Mol Med 28: 258-269, 2022.
12. Liu LL, Han Y, Zhang ZJ, Wang YQ, Hu YW, Kaznacheyeva E, Ding JQ, Guo DK, Wang GH, Li B and Ren HG: Loss of DJ-1 function contributes to Parkinson's disease pathogenesis in mice via RACK1-mediated PKC activation and MAO-B upregulation. Acta Pharmacol Sin 44: 1948-1961, 2023.
13. Gu C, Zhang Y, Hu Q, Wu J, Ren H, Liu CF and Wang G: P7C3 inhibits GSK3β activation to protect dopaminergic neurons against neurotoxin-induced cell death in vitro and in vivo. Cell Death Dis 8: e2858, 2017.
14. Livak KJ and Schmittgen TD: Analysis of relative gene expression data using real-time quantitative PCR and the 2(-Delta Delta C(T)) method. Methods 25: 402-408, 2001.
15. Nagatsu T and Nagatsu I: Tyrosine hydroxylase (TH), its cofactor tetrahydrobiopterin (BH4), other catecholamine-related enzymes, and their human genes in relation to the drug and gene therapies of Parkinson's disease (PD): Historical overview and future prospects. J Neural Transm (Vienna) 123: 1255-1278, 2016.
16. Kordower JH, Olanow CW, Dodiya HB, Chu Y, Beach TG, Adler CH, Halliday GM and Bartus RT: Disease duration and the integrity of the nigrostriatal system in Parkinson's disease. Brain 136: 2419-2431, 2013.
17. Zheng J and Conrad M: The metabolic underpinnings of ferroptosis. Cell Metab 32: 920-937, 2020.
18. Yu H, Chang Q, Sun T, He X, Wen L, An J, Feng J and Zhao Y: Metabolic reprogramming and polarization of microglia in Parkinson's disease: Role of inflammasome and iron. Ageing Res Rev 90: 102032, 2023.
19. Patani R, Hardingham GE and Liddelow SA: Functional roles of reactive astrocytes in neuroinflammation and neurodegeneration. Nat Rev Neurol 19: 395-409, 2023.
20. Kwon HS and Koh SH: Neuroinflammation in neurodegenerative disorders: The roles of microglia and astrocytes. Transl Neurodegener 9: 42, 2020.
21. Mitchell JP and Carmody RJ: NF-κB and the transcriptional control of inflammation. Int Rev Cell Mol Biol 335: 41-84, 2018.
22. Lee J and Hyun DH: The interplay between intracellular iron homeostasis and neuroinflammation in neurodegenerative diseases. Antioxidants (Basel) 12: 918, 2023.
23. Wang Y, Wu S, Li Q, Sun H and Wang H: Pharmacological inhibition of ferroptosis as a therapeutic target for neurodegenerative diseases and strokes. Adv Sci (Weinh) 10: e2300325, 2023.
24. Tansey MG, Wallings RL, Houser MC, Herrick MK, Keating CE and Joers V: Inflammation and immune dysfunction in Parkinson disease. Nat Rev Immunol 22: 657-673, 2022.
25. Zhang W, Xiao D, Mao Q and Xia H: Role of neuroinflammation in neurodegeneration development. Signal Transduct Target Ther 8: 267, 2023.
26. Isik S, Yeman Kiyak B, Akbayir R, Seyhali R and Arpaci T: Microglia mediated neuroinflammation in Parkinson's disease. Cells 12: 1012, 2023.
27. Angelova PR, Choi ML, Berezhnov AV, Horrocks MH, Hughes CD, De S, Rodrigues M, Yapom R, Little D, Dolt KS, *et al*: Alpha synuclein aggregation drives ferroptosis: An interplay of iron, calcium and lipid peroxidation. Cell Death Differ 27: 2781-2796, 2020.
28. Dixon SJ, Lemberg KM, Lamprecht MR, Skouta R, Zaitsev EM, Gleason CE, Patel DN, Bauer AJ, Cantley AM, Yang WS, *et al*: Ferroptosis: An iron-dependent form of nonapoptotic cell death. Cell 149: 1060-1072, 2012.
29. Shibu MA, Bharath M and Velmurugan BK: Regulating inflammation associated ferroptosis - A treatment strategy for Parkinson disease. Curr Med Chem 28: 6895-6914, 2021.
30. Grubbauer HM, Dornbusch HJ, Dittrich P, Weippl G, Mutz I, Zobel G, Georgopoulos A and Fotter R: Ceftriaxone monotherapy for bacterial meningitis in children. Chemotherapy 36: 441-447, 1990.
31. Rothstein JD, Patel S, Regan MR, Haenggeli C, Huang YH, Bergles DE, Jin L, Dykes Hoberg M, Vidensky S, Chung DS, *et al*: Beta-lactam antibiotics offer neuroprotection by increasing glutamate transporter expression. Nature 433: 73-77, 2005.

32. Pajarillo E, Rizor A, Lee J, Aschner M and Lee E: The role of astrocytic glutamate transporters GLT-1 and GLAST in neurological disorders: Potential targets for neurotherapeutics. Neuropharmacology 161: 107559, 2019.
33. Malik AR and Willnow TE: Excitatory amino acid transporters in physiology and disorders of the central nervous system. Int J Mol Sci 20: 5671, 2019.
34. Abulseoud OA, Alasmari F, Hussein AM and Sari Y: Ceftriaxone as a novel therapeutic agent for hyperglutamatergic states: Bridging the gap between preclinical results and clinical translation. Front Neurosci 16: 841036, 2022.
35. Gao J, Liu L, Liu C, Fan S, Liu L, Liu S, Xian XH and Li WB: GLT-1 knockdown inhibits ceftriaxone-mediated improvements on cognitive deficits, and GLT-1 and xCT expression and activity in APP/PS1 AD mice. Front Aging Neurosci 12: 580772, 2020.
36. Rao PSS, Saternos H, Goodwani S and Sari Y: Effects of ceftriaxone on GLT1 isoforms, xCT and associated signaling pathways in P rats exposed to ethanol. Psychopharmacology (Berl) 232: 2333-2342, 2015.
37. Lewerenz J, Albrecht P, Tien ML, Henke N, Karumbayaram S, Kornblum HI, Wiedau-Pazos M, Schubert D, Maher P and Methner A: Induction of Nrf2 and xCT are involved in the action of the neuroprotective antibiotic ceftriaxone in vitro. J Neurochem 111: 332-343, 2009.
38. Patel SA, Warren BA, Rhoderick JF and Bridges RJ: Differentiation of substrate and non-substrate inhibitors of transport system xc(-): An obligate exchanger of L-glutamate and L-cystine. Neuropharmacology 46: 273-284, 2004.
39. Dar NJ, John U, Bano N, Khan S and Bhat SA: Oxytosis/ferroptosis in neurodegeneration: The underlying role of master regulator glutathione peroxidase 4 (GPX4). Mol Neurobiol 61: 1507-1526, 2024.
40. Liu Y, Wan Y, Jiang Y, Zhang L and Cheng W: GPX4: The hub of lipid oxidation, ferroptosis, disease and treatment. Biochim Biophys Acta Rev Cancer 1878: 188890, 2023.
41. Sun S, Shen J, Jiang J, Wang F and Min J: Targeting ferroptosis opens new avenues for the development of novel therapeutics. Signal Transduct Target Ther 8: 372, 2023.
42. Wang Y, Lv MN and Zhao WJ: Research on ferroptosis as a therapeutic target for the treatment of neurodegenerative diseases. Ageing Res Rev 91: 102035, 2023.
43. Jiang X, Wu K, Ye XY, Xie T, Zhang P, Blass BE and Bai R: Novel druggable mechanism of Parkinson's disease: Potential therapeutics and underlying pathogenesis based on ferroptosis. Med Res Rev 43: 872-896, 2023.
44. Smaga I, Fierro D, Mesa J, Filip M and Knackstedt LA: Molecular changes evoked by the beta-lactam antibiotic ceftriaxone across rodent models of substance use disorder and neurological disease. Neurosci Biobehav Rev 115: 116-130, 2020.
45. Ritter K, Somnuke P, Hu L, Griemert EV and Schäfer MKE: Current state of neuroprotective therapy using antibiotics in human traumatic brain injury and animal models. BMC Neurosci 25: 10, 2024.
46. Zhang Y, Zhang X and Qu S: Ceftriaxone protects astrocytes from MPP(+) via suppression of NF-κB/JNK/c-Jun signaling. Mol Neurobiol 52: 78-92, 2015.
47. Zhou X, Lu J, Wei K, Wei J, Tian P, Yue M, Wang Y, Hong D, Li F, Wang B, *et al*: Neuroprotective effect of ceftriaxone on MPTP-induced parkinson's disease mouse model by regulating inflammation and intestinal microbiota. Oxid Med Cell Longev 2021: 9424582, 2021.
48. Tieu K: A guide to neurotoxic animal models of Parkinson's disease. Cold Spring Harb Perspect Med 1: a009316, 2011.
49. Mao Q, Qin WZ, Zhang A and Ye N: Recent advances in dopaminergic strategies for the treatment of Parkinson's disease. Acta Pharmacol Sin 41: 471-482, 2020.
50. Jackson-Lewis V and Przedborski S: Protocol for the MPTP mouse model of Parkinson's disease. Nat Protoc 2: 141-151, 2007.
51. Narmashiri A, Abbaszadeh M and Ghazizadeh A: The effects of 1-methyl-4-phenyl-1,2,3,6-tetrahydropyridine (MPTP) on the cognitive and motor functions in rodents: A systematic review and meta-analysis. Neurosci Biobehav Rev 140: 104792, 2022.
52. Ge J, Lin H, Yang J, Li Q, Zhou J, Qin Z and Wu F: TP53-induced glycolysis and apoptosis regulator (TIGAR) ameliorates lysosomal damage in the 1-methyl-4-phenyl-1, 2, 3, 6-tetrahydropyridine-mediated mouse model of Parkinson's disease. Toxicol Lett 339: 60-69, 2021.
53. Guo DK, Zhu Y, Sun HY, Xu XY, Zhang S, Hao ZB, Wang GH, Mu CC and Ren HG: Pharmacological activation of REV-ERBα represses LPS-induced microglial activation through the NF-κB pathway. Acta Pharmacol Sin 40: 26-34, 2019.
54. He J, Zhu G, Wang G and Zhang F: Oxidative stress and neuroinflammation potentiate each other to promote progression of dopamine neurodegeneration. Oxid Med Cell Longev 2020: 6137521, 2020.
55. Mohan S, Alhazmi HA, Hassani R, Khuwaja G, Maheshkumar VP, Aldahish A and Chidambaram K: Role of ferroptosis pathways in neuroinflammation and neurological disorders: From pathogenesis to treatment. Heliyon 10: e24786, 2024.